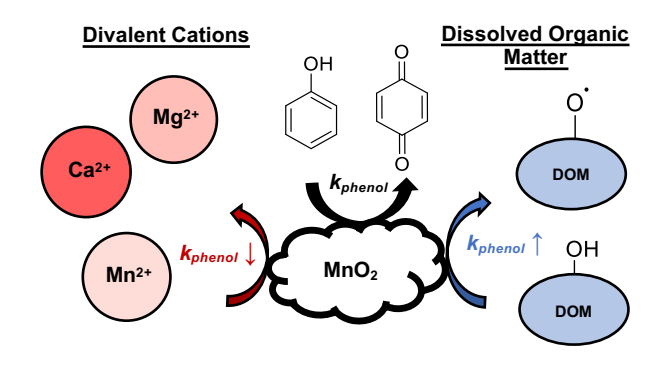
- The influence of divalent cation inhibition and dissolved organic
- 2 matter enhancement on phenol kinetics by manganese oxides

3	Jenna T. Swenson, Matthew Ginder-Vogel, 1,2† and Christina K. Remucal 1,2*					
4						
5	¹ Environmental Chemistry and Technology					
6	University of Wisconsin - Madison					
7	Madison, Wisconsin					
8	² Dept. of Civil and Environmental Engineering					
9	University of Wisconsin - Madison					
10	Madison, Wisconsin					
11						
12						
13	† Corresponding author address: 660 N. Park St., Madison, WI 53706; e-mail:					
14	mgindervogel@wisc.edu; telephone: (608) 262-0768					
15						
16	* Corresponding author address: 660 N. Park St., Madison, WI 53706; e-mail: remucal@wisc.edu;					
17	telephone: (608) 262-1820					
18						

19 For Table of Contents Only



Abstract

22

23

24

25

26

27

28

29

30

31

32

33

34

35

36

37

38

39

Manganese oxides can oxidize organic compounds such as phenols and may potentially be used in passive water treatment applications. However, the impact of common water constituents, including cations and dissolved organic matter (DOM), on this reaction is poorly understood. For example, the presence of DOM can either increase or decrease phenol oxidation rates by manganese oxides. Furthermore, the interactions of DOM and cations and their impact on phenol oxidation rates have not been examined. Therefore, we investigated the oxidation kinetics of six phenolic contaminants with acid birnessite in ten whole water samples. The oxidation rate constants of 4-chlorophenol, 4-tert-octylphenol, 4-bromophenol, and phenol consistently decreased in all waters relative to buffered ultrapure water, whereas the oxidation rate of bisphenol A and triclosan increased by up to 260% in some waters. Linear regression analyses and targeted experiments demonstrated that inhibition of phenol oxidation is largely determined by cations. Furthermore, quencher experiments indicated that radical-mediated interactions from oxidized DOM contributed to enhanced oxidation of bisphenol A. The variable changes between compounds and water samples demonstrate the challenge of accurately predicting contaminant transformation rates in environmentally relevant systems based on experiments conducted in the absence of natural water constituents.

40	Key	Words	5
----	-----	-------	---

41 Manganese oxides, phenolic contaminants, dissolved organic matter, cations, oxidation

42

43 Synopsis

- Rate of phenolic contaminant oxidation by manganese oxides is determined by the contaminant
- and water chemistry, with implications for predicting contaminant lifetimes in complex systems.

Introduction

Manganese(III/IV) oxides are naturally occurring, redox active minerals that can oxidize inorganic^{1–3} and organic contaminants^{1,4–10} in the environment. Furthermore, manganese oxides can be used in water treatment systems to transform contaminants like phenols.^{4–6,11–13} Phenolic contaminants, such as bisphenol A and triclosan, are found in landfill leachate, surface waters, and wastewaters due to their presence in consumer products and industrial applications.^{14–18} Some phenols are endocrine disruptors (e.g. bisphenol A) or mutagenic (e.g. triclosan) and may pose a threat to environmental health.^{19,20}

The oxidation mechanism for phenolic compounds by manganese oxides in model systems (i.e., buffered ultrapure water) is well established. First, the phenol sorbs to the mineral surface where it undergoes a one-electron transfer and forms a phenoxy radical. Next, the phenoxy radical can desorb from the mineral surface and form polymeric products via radical coupling or undergo a second one-electron transfer at the mineral surface to produce aqueous Mn(II) and benzoquinone products (**Supporting Information Figure S1**).^{4,5,8,11,21}

Other species present in environmentally relevant systems can influence the oxidation rate of phenols by manganese oxides. For example, inorganic cations generally decrease the oxidation rate of organic compounds. 9,10,13,22–30 The degree of inhibition depends on cation type as divalent cations (e.g., Ca²⁺, Mg²⁺, Mn²⁺) have a larger inhibitory effect than monovalent cations (e.g., Na⁺). 13,26–28 This trend is attributable to stronger sorption of divalent cations to manganese oxide surfaces compared to monovalent cations. 13,26,31 Furthermore, divalent cations can interact with other organic compounds in solution, such as dissolved organic matter (DOM), to form complexes or increase DOM sorption to the mineral surface (**Figure S1**). 32–37

DOM is a mixture of organic molecules found in natural and engineered systems^{38–43} and can also impact phenolic compound oxidation by manganese oxides. DOM can increase, decrease, or have little effect on contaminant oxidation rates (Table S1). For example, DOM can increase or decrease triclosan oxidation rates depending on its concentration and composition. 25,44,45 Similarly, the presence of the same organic matter can increase¹³ or decrease²³ the rate of bisphenol A oxidation. It is possible that DOM slows the oxidation of other organic species by competing for manganese oxide surface sites 10,25,29,45-52 or by reductive dissolution of the mineral. 4,8,53,54 Conversely, the mechanisms of rate enhancement for phenolic compound oxidation by DOM have not been well examined. The rate enhancement of sulfonamide oxidation by manganese oxides with organic matter and model compounds was attributed to radical-mediated interactions. 55,56 Similarly, the rate enhancement of phenolic compound mixtures was attributed to radical-mediated interactions based on quenching experiments.⁵⁷ While DOM is suspected to be oxidized primarily via phenolic moieties, 38,52,58-60 evidence for this mechanism of rate enhancement for phenolic compounds with organic matter is lacking. Furthermore, it is challenging to identify the mechanisms leading to inhibition or enhancement due to variability in experimental conditions (e.g., organic carbon concentration, pH, manganese oxide type; **Table S1**) and lack of DOM composition data. We hypothesize that the composition of DOM influences its ability to either increase or

69

70

71

72

73

74

75

76

77

78

79

80

81

82

83

84

85

86

87

88

89

90

91

We hypothesize that the composition of DOM influences its ability to either increase or decrease phenol compound oxidation rates. DOM composition is a function of source inputs and environmental processing and therefore can vary widely within the same water body or across different systems. DOM composition influences its reactivity with sunlight, 40,41,63-65 chemical disinfectants (e.g., chlorine and ozone), 66-71 and manganese oxides. For example, highly aromatic DOM undergoes greater changes following oxidation with manganese oxides than more

aliphatic DOM.^{38,58} This composition-dependent transformation means DOM from different environmental systems (e.g., wastewater vs. dystrophic lakes) likely results in divergent impacts on the oxidation of phenolic contaminants by manganese oxides; however, no study has yet provided evidence for this relationship.

The aim of this study is to investigate how DOM composition and DOM interactions with cations influence the oxidation kinetics of six phenolic contaminants (i.e., bisphenol A, triclosan, 4-chlorophenol, 4-tert-octylphenol, 4-bromophenol, phenol) with manganese oxides. These six compounds were chosen as they range in acid dissociation constants (pKa), energy of the highest occupied molecular orbital (EHOMO), and one-electron oxidation potentials (Eox; **Table S2**.)6,72–76 We use water samples collected from lakes with varying trophic status, rivers with differing DOM inputs, and wastewater effluent. These samples range widely in DOM composition and in cation concentration. We use linear regression modeling to investigate the role of DOM composition and cation concentrations on phenol oxidation kinetics and conduct targeted experiments to identify the mechanisms of rate suppression and enhancement. The results of this study have implications for predicting phenolic contaminant fate in environmental systems, as well as for designing effective manganese-mediated water treatment strategies.

Materials and Methods

Materials. Two batches of acid birnessite were synthesized as previously described^{38,77} and confirmed to be acid birnessite by X-ray diffraction (XRD; **Figure S2**). Both minerals had an average oxidation state of 4.0 ± 0.01 measured by oxalate titration.⁷⁸ All other chemicals were used as received (**Section S3**).

Table 1. Characteristics of the water samples used in this study. DOM bulk characteristics include E_2 : E_3 , $SUVA_{254}$, fluorescence index, and electron-donating capacity. The total divalent cation concentrations are of those found in the diluted whole water samples, with the undiluted concentrations listed in parentheses, and are the sum of total Ca, Mg, and Mn concentrations. Error associated with electron-donating capacity is the standard deviation of replicate measurements (n = 4, *n = 3).

Water Sample	E ₂ :E ₃	SUVA ₂₅₄ (L mg- C ⁻¹ m ⁻¹⁾	Fluorescence Index	Electron- Donating Capacity (mmol e ⁻ g-C ⁻¹)	Total Divalent Cations (mM)
Nine Springs Secondary Effluent (WW1)	4.6	2.6	2.02	3.22 ± 0.34	1.73 (3.17)
Badfish Creek CE ³⁸ (WW2)	7.2	2.3	1.96	2.41 ± 0.19	2.35 (3.38)
Trout Lake (OL1)	5.7	1.0	1.52	0.68 ± 0.14	0.40 (0.40)
Big Muskellunge Lake (OL2)	10.3	0.8	1.62	$0.41 \pm 0.02*$	0.15 (0.22)
Seven Island Lake ³⁸ (ML1)	8.9	2.0	1.57	1.25 ± 0.18	0.17 (0.19)
Lake Ivanhoe ³⁸ (EL1)	5.9	3.8	1.51	0.33 ± 0.02	0.59 (2.04)
Sand Creek ^{38,40} (R1)	4.2	4.8	1.41	1.34 ± 0.21	0.03 (0.47)
Blatnik Bridge ^{38,40} (R2)	4.7	3.7	1.57	1.83 ± 0.06	0.13 (0.63)
Trout Bog (DL1)	5.1	4.7	1.40	1.81 ± 0.11	0.01 (0.04)
Crystal Bog (DL2)	4.8	3.0	1.46	2.13 ± 0.13	0.01 (0.03)
Park Point West (EL2)	5.5	2.8	1.54	1.59 ± 0.14	0.25 (0.39)
Lake Wingra (EL3)	7.0	1.9	1.61	0.66 ± 0.13*	1.06 (1.84)

Water samples. Twelve surface water samples were collected from Minnesota and Wisconsin, USA (Tables 1 and S4). Samples included wastewater effluent (WW1 and WW2), rivers (R1 and R2), and oligotrophic (OL1 and OL2), eutrophic (EL1, EL2, EL3), mesotrophic (ML1), and dystrophic (DL1 and DL2) lakes. Water samples from EL2 and EL3 were tested with a subset of target compounds due to limited sample quantity. Samples were filtered (0.45 µm, nylon) immediately after collection and stored in amber glass bottles at 4°C. Samples were refiltered (0.22 µm, nylon) 24 hours prior to reactions and analyses; therefore, the operational definition of DOM in this study is organic matter that passes through a 0.22 um filter. Dissolved organic carbon (DOC) was measured using a total organic carbon analyzer. DOM composition was assessed using UV-vis spectroscopy, fluorescence spectroscopy, and electron donating capacity (EDC) measurements (Section S4). Specific UV absorption at 254 nm (SUVA₂₅₄) was calculated by dividing absorbance at 254 nm by [DOC]. The ratio of absorbances at 250 nm to 365 nm for each whole water sample was used to determine E₂:E₃.80 The fluorescence index was determined as the ratio of emission intensities at 470 nm and 520 nm at an excitation wavelength of 370 nm. 81-83 Inorganic water chemistry (i.e., alkalinity and ions) was characterized as described in **Section S4**.

122

123

124

125

126

127

128

129

130

131

132

133

134

135

136

137

138

139

140

141

142

143

144

Kinetic batch reactions. Reaction kinetics of the six phenolic compounds with acid birnessite in the presence and absence of whole water samples were assessed using batch reactors. Bisphenol A, triclosan, 4-*tert*-octylphenol, 4-chlorophenol, 4-bromophenol, and phenol were selected based on their expected differences in reactivity due to differences in molecular structure.⁶ Water samples were diluted to a consistent [DOC] equal to the lowest carbon water (i.e., 3.54 mg-C/L in OL1) because increasing [DOC] can increase the inhibition of organic contaminant transformation by manganese oxides.^{9,24,25,45,46} Each diluted water sample was amended with 5

mM acetate buffer and 10 μ M of the phenolic compound in a separate vessel prior to reaction, with analogous control experiments conducted with 5 mM acetate in ultrapure water. Target compounds did not degrade in the absence of acid birnessite (**Figure S3**). Acid birnessite was added (final concentration = 0.39 mM Mn) after being rehydrated overnight in 1 mL of 5 mM acetate buffer. These concentrations resulted in a 3:4 C:Mn molar ratio, representative of DOC and manganese concentrations found in Mn-rich environments.^{38,84} Due to the strong pH dependence of these reactions, ^{4,13,15,22–25,44} 5 mM acetate buffer was used at a starting pH of 5.5 \pm 0.1 This pH is below the pK_a values of the target phenols (range: 7.7 – 10.2; **Table S2**).

Reactions were initiated by adding the buffered water sample and target compound mixture to the rehydrated acid birnessite. Reactors were constantly stirred at 350 rpm in the dark. Sample aliquots (280 μ L) were quenched with 20 μ L of 20 mM L-ascorbic acid. The pH at the end of each reaction increased by \leq 0.5 pH units. Target compounds were quantified in the quenched samples using high-performance liquid chromatography (HPLC; **Section S5**). Concentration data was fit assuming pseudo-first-order kinetics (**Figure S4**) as observed previously.^{4,6,44,57} Production of aqueous Mn after reaction could not be detected within instrumental error (i.e., 5% RSD). All kinetics experiments were conducted in triplicate and error bars represent the propagated standard error of the linear regression from replicates.

Additional batch reactions were conducted to investigate the effects of divalent cations on the oxidation of bisphenol A and 4-chlorphenol with acid birnessite in the presence and absence of DOM from DL1. All other experimental conditions were the same as the reactions described above. Divalent cation concentrations of Mn²⁺, Ca²⁺, and Mg²⁺ were equal to those of the undiluted water samples from R1, EL1, and WW2 (**Tables 1** and **S7**) and were added as chloride salts. DOM-free controls with divalent cations were run under the same conditions alongside samples

containing divalent cations and DL1 water. Anions were not considered due to repulsive electrostatic interactions between the negatively charged acid birnessite and anions. 26,28,85,86

Kinetic reactions using a nonspecific radical quencher *tert*-butanol^{87–91} were conducted to explore the role of radical-mediated reactions in enhancing the rate of bisphenol A oxidation using water samples from DL1, DL2, and WW1. *tert*-Butanol (50 mM) was used as it is not likely to react with manganese oxides and does not alter the mineral surface.⁵⁷ The dystrophic lake samples were used in these experiments because bisphenol A oxidation rate enhancement was observed in these samples as described below. Water from WW1 was used as a control because bisphenol A degradation decreased in this sample and no substantial effect from radical reactions was expected.

Linear regression analysis. Linear regression models were constructed to assess correlations between the observed changes in pseudo-first-order reaction rates of each target compound with DOM compositional parameters (i.e., fluorescence index, SUVA₂₅₄, E₂:E₃, and EDC) and total divalent cation concentrations in the reactors. Normality of the outcome variable $(k_{\text{sample}} / k_{\text{control}})$ was tested using the Shapiro-Wilk test. The distribution of reaction rate ratios for some target compounds were found to be non-normally distributed and therefore a log-transformation was performed on all data to maintain consistent parameters between compounds. Correlations were considered significant when p < 0.05.

Results and Discussion

Reactivity of target compounds in the whole water samples. The baseline reactivity of the six target compounds with acid birnessite was determined by quantifying pseudo-first-order rate constants in acetate-buffered (pH 5.5) ultrapure water (**Figure S4**; **Table S2**). The order of reactivity from most to least reactive was 4-*tert*-octylphenol > triclosan > bisphenol A > 4-

bromophenol > 4-chlorophenol > phenol, with half-lives ranging from 0.4 - 5.8 hours. We explored trends in reactivity by plotting measured reaction rates against available phenol descriptor data including pK_a values, E_{HOMO} , and E_{ox} (**Figure S5**; **Table S9**). Compounds with electron-withdrawing substituents have lower pK_a values and are slower to react due to decreased electron density. $^{6,72-75}$ E_{HOMO} is related to ionization potential and compounds with higher E_{HOMO} values have faster oxidation rates as the energy required to lose an electron is lower. 6,73,75,76 Conversely, larger E_{ox} values are correlated with lower oxidation rates as the energy required to lose the first electron becomes greater, making it more difficult to be oxidized by the manganese oxide. There were no statistically significant correlations for these parameters for the six studied phenols (**Table S9**). Furthermore, accurate QSAR modeling requires a much larger sample size than used in this study. 6,92,93

The oxidation rate constants of four of the six target compounds (i.e., 4-chlorophenol, 4tert-octylphenol, phenol, and 4-bromophenol) were consistently slower in the presence of water
from natural and engineered aquatic systems compared to buffered ultrapure water controls
(Figure 1c - 1f; Tables S10 and S11). However, the extent of inhibition varied with water type.
For example, the oxidation rate constants were slowest in wastewater samples, with an average decrease of $97 \pm 3\%$ for eight contaminant/water pairs. In contrast, dystrophic lake samples had the least impact on the oxidation rates of these four compounds, which decreased by 14 - 63% relative to the controls. Variable changes to oxidation rates were observed with water samples collected from the rivers and other lakes.

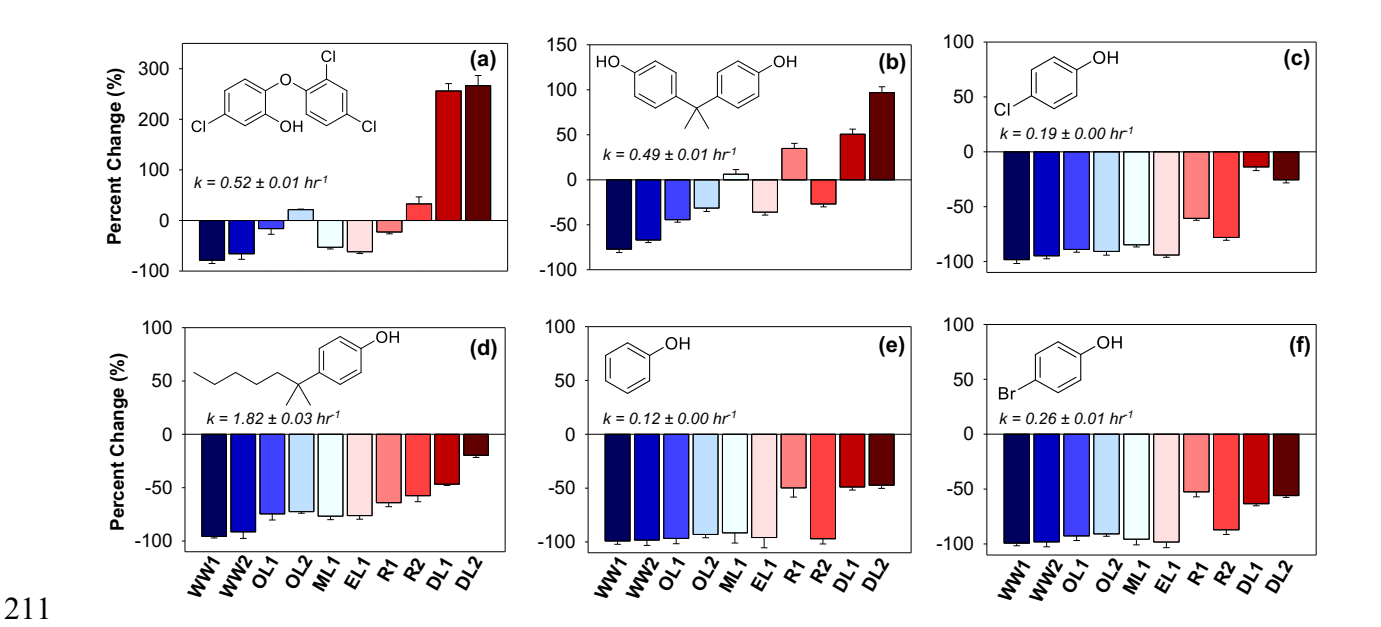


Figure 1. Percent change of target compound pseudo-first-order oxidation rate in the presence of whole water samples relative to the rate measured in a buffered, ultrapure control for (a) triclosan, (b) bisphenol A, (c) 4-chlorophenol, (d) 4-*tert*-octylphenol, (e) phenol, and (f) 4-bromophenol with 1.70 mg acid birnessite (0.39 mM-Mn) in ten whole water samples (3.54 mg-C/L, pH 5.5). Error bars represent the propagated standard error associated with the pseudo-first-order rates in the presence and absence of whole water constituents. The rate constant listed below each target compound structure is the average rate constant of replicate measurements (n ≥ 6) in a buffered (pH = 5.5), ultrapure water control with acid birnessite (0.39 mM-Mn). The associated error is the propagated standard error the pseudo-first-order rate constants. Note the different y-axis scales in panels (a) and (b) compared to panels (c) − (f).

In contrast to the four simple phenols, bisphenol A and triclosan oxidation rate constants were slower in some water samples and faster in other water samples relative to buffered ultrapure water controls (**Figures 1a – 1b**; **Tables S10** and **S11**). The largest decreases in bisphenol A and triclosan oxidation rate constants were observed in wastewater samples (i.e., 66 – 78% compared to the controls), which were similar to the decreases observed for the four simple phenols. However, increased oxidation rate constants of both bisphenol A and triclosan were observed in dystrophic lake samples. For example, the oxidation rate constant of bisphenol A was enhanced by 51 and 97% in the two dystrophic lake samples, while triclosan was enhanced by >250% in

both. Oxidation rates increased in individual river and lake samples. The bisphenol A oxidation rate constant was 6 and 35% faster in samples ML1 and R1, respectively. Similarly, the triclosan oxidation rate constant was 22 and 33% faster in samples OL2 and R2, respectively.

Linear regression analysis of water chemistry parameters. We first used linear regression analysis to investigate which water constituents were responsible for the observed changes in phenol oxidation kinetics. We selected independent variables that separately assessed the impact of divalent cations and DOM on contaminant oxidation kinetics by manganese oxides. For example, individual divalent cations consistently decrease the oxidation rate of organic compounds, including bisphenol A and triclosan, by these redox active minerals. 9,10,13,22–30,44 Divalent cations are thought to slow phenolic compound oxidation by two mechanisms (Figure S1). First, divalent cations can occupy vacancy sites on the manganese oxide surface, thereby blocking the target compound from the mineral surface. 13,22,23,25,29,33,94,95 Second, divalent cations may accumulate at the mineral surface, potentially altering characteristics of the mineral and preventing oxidation. Thus, we hypothesized that interference from divalent cations contributed to the decrease in oxidation rate constants (Figure 1).

All target compounds, except for phenol, had a statistically significant (p < 0.05) negative correlation with the diluted divalent cation concentrations (i.e., Ca^{2+} , Mg^{2+} , Mn^{2+} ; **Figure 2b**; **Table S12**). These correlations were consistent with the slower oxidation rates observed in water samples containing higher divalent cation concentrations (e.g., wastewaters). While this result potentially explained the 59 out of 67 cases where phenol oxidation rate constants decreased in whole water samples, lower cation concentration did not explain the cases where faster oxidation rate constants were observed (e.g., bisphenol A and triclosan in dystrophic lakes).

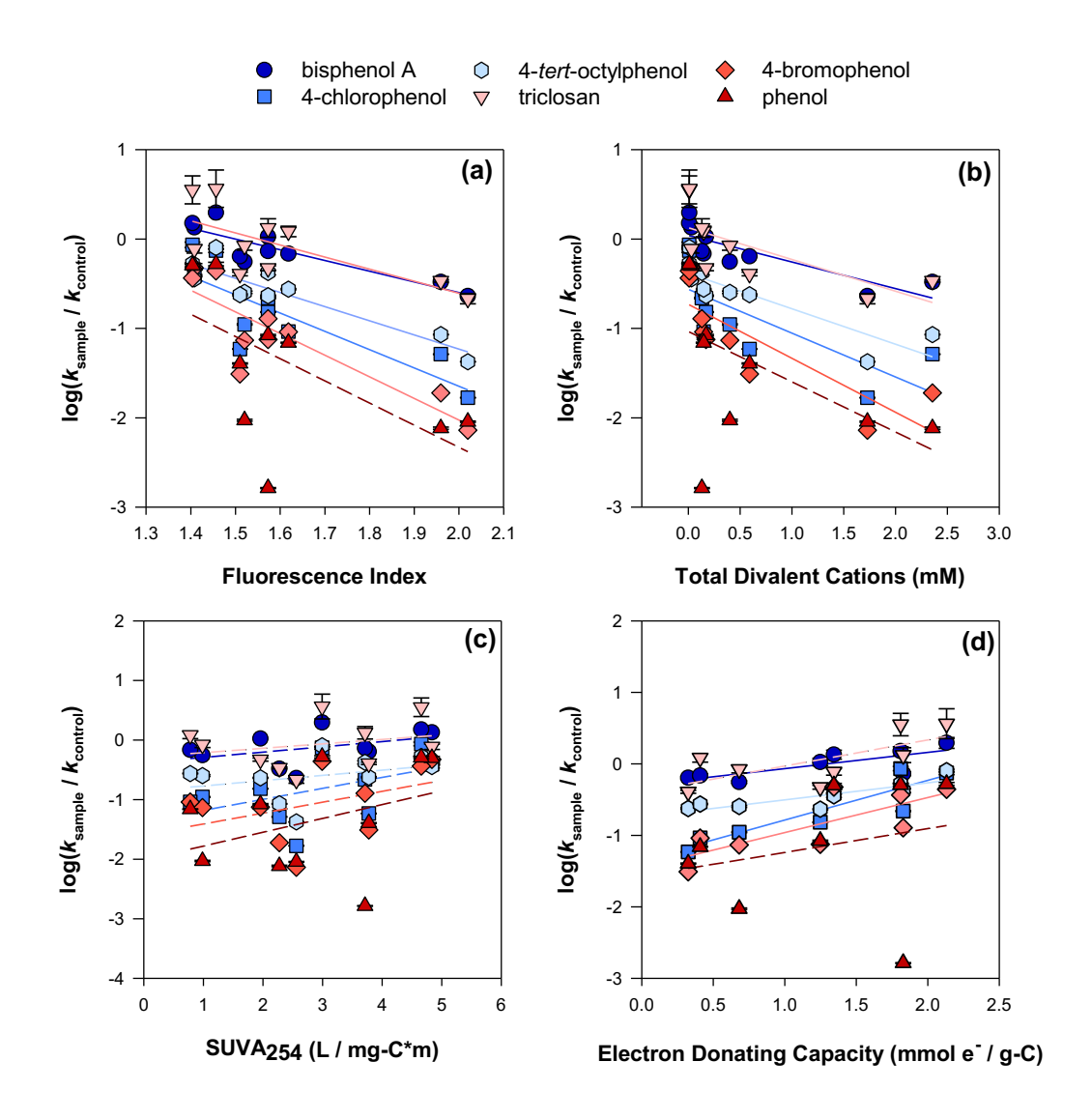


Figure 2. Single linear regression models of changes in the pseudo-first-order rate constants for the six target compounds relative to the buffered, ultrapure control with (a) fluorescence index, (b) the diluted sample concentrations of total divalent cations $(Ca^{2+}, Mg^{2+}, Mn^{2+})$, (c) SUVA₂₅₄, and (d) electron donating capacity excluding the two wastewater samples. Error bars represent the propagated standard error of the pseudo-first-order rate constants of triplicate reactors. Solid lines represent statistically significant (p < 0.05) correlations, while dashed lines are statistically insignificant. Regression statistics are provided in **Table S12**.

We hypothesized that DOM led to increased oxidation rates in some cases and the extent of impact was attributable to the initial DOM composition. This hypothesis was based on findings in studies that investigated the impact of DOM on contaminant oxidation in the absence of cations,

in addition to studies that focused on DOM reactivity with manganese oxides. 32,33,38,58,59 DOM has been shown to both increase and decrease organic compound oxidation by manganese oxides (Table S1), although the mechanism of these interactions has not been investigated. For example, bisphenol A oxidation can increase¹³ or decrease^{15,23,29} in the presence of DOM, in agreement with the results of this study (**Figure 1b**). Furthermore, DOM contains redox active functional groups, including phenols, that react directly with manganese oxides and may result in the formation of phenolic radicals and mineral surface modification. Common bulk characteristics of DOM, including apparent molecular weight, aromaticity, and phenolic content have been correlated with the reactivity of DOM with manganese oxides. 32,38,58,59,96 Therefore, we tested for correlations between changes in oxidation rate constants and carbon-normalized DOM compositional parameters. These parameters included SUVA₂₅₄, which is correlated with DOM aromaticity, ^{41,79} and E₂:E₃, which is inversely related to direct measurements of molecular weight. 41,43,80 Fluorescence index was used to characterize the source inputs of DOM; low values correspond to terrestrially derived DOM, while higher values correspond to microbially derived DOM. 81,82 EDC is associated with the phenolic content of DOM in natural waters.⁹⁷

264

265

266

267

268

269

270

271

272

273

274

275

276

277

278

279

280

281

282

283

284

285

286

All target compounds, except for phenol, had significant negative correlations with fluorescence index (**Figure 2a**; **Table S12**). These correlations suggested characteristics of DOM composition related to source inputs were important for determining changes to the oxidation rates for many phenolic compounds. Specifically, DOM with lower fluorescence index values (i.e., indicative of primarily terrestrial inputs)^{43,81,98,99} was more likely to enhance oxidation rates. Although not statistically significant, a positive trend with SUVA₂₅₄ was observed for all target compounds (**Figure 2c**) and complimented the fluorescence index correlation because more aromatic DOM is typically of terrestrial origin.^{64,100–102} When all water samples were included in

the EDC regression, a statistically insignificant negative trend was observed (**Figure S7a**; **Table S12**). The divergent trends in SUVA₂₅₄ and EDC were unexpected since these two parameters are often correlated.^{63,103} This trend in EDC regression was attributed to the inclusion of wastewater samples as these have confounding variables (i.e., enriched hetero-atom containing functional groups, high concentrations of metals and ions) that contribute to the measured EDC.⁶³ When wastewater samples were excluded, all target compounds had positive trends with EDC; these trends were statistically significant for bisphenol A, 4-chlorophenol, 4-*tert*-octylphenol, and 4-bromophenol (**Figure 2d**; **Table S12**). These trends indicated that phenolic-rich DOM in natural water samples is more likely to enhance phenol oxidation and the composition of DOM influences its impact on phenol oxidation kinetics by manganese oxides. No compounds had significant correlations with E₂:E₃ (**Figure S7b**; **Table S12**).

The linear regression results showed the kinetics of five of the target compounds were correlated with both divalent cation concentration and with DOM composition parameters. However, this analysis did not allow us to determine which factor was dominant or to identify how their combination impacted the overall measured changes in rate constants. The combined influence of cations and DOM was important to consider because both species were present in the whole water samples and always co-occur in the environment. Divalent cations can enhance DOM sorption to the manganese oxide surface via ligand-exchange or cation-bridging mechanisms^{33–37} and could affect phenolic compound kinetics in two ways (**Figure S1**). First, enhanced sorption of DOM to the manganese oxide surface may block reactive sites from phenolic target compounds because DOM is thought to sorb and react via phenolic moieties;^{38,52,58–60} thus, competitive sorption could result in slower removal of the target compound. Second, enhanced DOM sorption to the mineral surface could result in increased oxidation of DOM and an increase in radical

intermediates generated when phenolic moieties within DOM react with manganese oxides via a one-electron transfer (i.e., as observed for individual phenols^{4,5,8,11,21}). It is possible that radical intermediates could react with phenolic compounds in solution as observed in systems containing multiple phenolic contaminants⁵⁷ or sulfonamides and humic acids,^{55,56} thereby increasing observed target compound kinetics. To better understand the impact of divalent cations and DOM composition on phenolic compound oxidation kinetics, we conducted kinetics experiments targeted at elucidating the mechanisms of inhibition and enhancement driven by divalent cations and DOM.

Influence of divalent cations and DOM interactions. The significant negative correlation for five of the target compounds with total divalent cations suggested an inhibitory mechanism driven by divalent cations. However, we could not distinguish between inhibition by cations and DOM because both species were present in all samples. Therefore, we investigated the impact of total divalent cations (i.e., Ca^{2+} , Mg^{2+} , Mn^{2+}) on bisphenol A and 4-chlorophenol oxidation kinetics through batch reactions with varying concentrations of total divalent cations, but with constant DOM concentration and composition. Bisphenol A and 4-chlorophenol were chosen for this subset of experiments because bisphenol A increased and decreased in oxidation rate, while 4-chlorophenol showed only decreases in rate constants in the initial kinetics testing (**Figure 1**). These experiments were conducted with 0.47 - 3.38 mM total divalent cations (i.e., the range in undiluted samples; **Table 1**) in buffered ultrapure water and water from sample DL1. The ratios of Ca^{2+} , Mg^{2+} , and Mn^{2+} used were the same as the undiluted water samples of R1, EL1, and WW2 (**Table S7**). DL1 water was chosen as it demonstrated high variability between compounds (e.g., enhancing bisphenol A oxidation but slowing 4-chlorophenol oxidation; **Figures**

1a and **1c**) and had a low concentration of total divalent cations (i.e., 0.01 mM in the diluted sample).

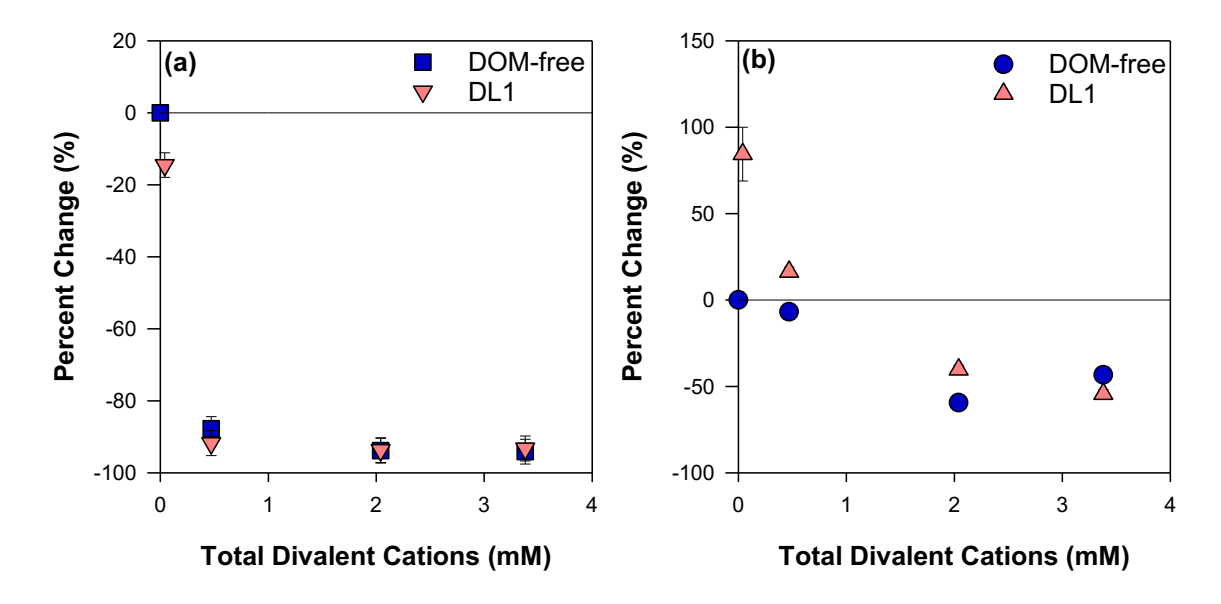


Figure 3. Percent change in pseudo-first-order reaction rates relative to the rate measured in a buffered, ultrapure control of DOM-free and DOM-containing systems with varying concentrations of divalent cations (Ca^{2+} , Mg^{2+} , Mn^{2+}) for (a) 4-chlorophenol and (b) bisphenol A. Systems with DOM used water from DL1 ([DOC] = 3.54 mg-C/L, pH = 5.5, 0.39 mM-Mn). Error bars are the propagated standard error of the pseudo-first-order rate constants of triplicate reactors; most error bars are smaller than the data points.

The oxidation rate constant of 4-chlorophenol decreased in both DOM-free and DL1 systems at all tested concentrations of total divalent cations (**Figure 3a**; **Tables S13** and **S14**). The decreases in 4-chlorophenol oxidation were nearly identical (p = 0.431, *t*-test) whether DOM was present or absent, decreasing between 88 and 94% relative to the control at all concentrations. The similarity between DOM-free and DL1 systems demonstrated that DOM interactions had a negligible impact on the oxidation of 4-chlorophenol when divalent cations were present. The dominance of cations in inhibiting the oxidation rate constants of 4-chlorophenol aligned with changes observed in initial kinetics testing for 4-chlorophenol. For example, wastewater samples

had the largest rate constant decreases and contained the highest divalent cation concentrations (**Figure 1c**; **Table 1**). Conversely, dystrophic lake samples contained the lowest divalent cation concentrations (**Table 1**) and resulted in the least impact to 4-chlorophenol oxidation (**Figure 1c**; **Table S11**).

Unlike 4-chlorophenol, the extent to which divalent cations slowed bisphenol A oxidation was dependent on the presence or absence of DOM (Figure 3b; Tables S13 and S14). With the addition of the lowest concentration of total divalent cations (0.47 mM), bisphenol A oxidation decreased by 7% in the DOM-free system. Conversely, at the same total divalent cation concentration, bisphenol A oxidation increased by 16% when DOM was added from DL1. The rate constant increase even in the presence of added divalent cations demonstrated that DOM interactions were responsible for bisphenol A rate enhancement. While higher divalent cations led to slower bisphenol A oxidation kinetics compared to control samples in both systems, a faster oxidation rate constant was observed in the presence of DOM at the moderate cation concentration (i.e., 2.04 mM) compared to the absence of DOM. At the highest cation concentration (3.38 mM), bisphenol A oxidation rates were similar regardless of the presence of DOM. Thus, DOM from DL1 increased the oxidation of bisphenol A at low to moderate cation concentrations, whereas cation inhibition became dominant at high divalent cation concentrations.

Evidence of radical-mediated rate enhancement. While regression analysis and divalent cation experiments revealed that rate inhibition was driven by divalent cations, these results did not explain the mechanism of rate enhancement observed in several cases (Figure 1). There were several lines of evidence that suggested DOM composition influenced bisphenol A oxidation. First, changes to the bisphenol A oxidation rate constants were negatively correlated with fluorescence index and positively correlated with EDC when the wastewaters were excluded

(**Figures 2a** and **2d**; **Table S12**). These significant correlations suggested DOM composed of primarily terrestrial inputs (i.e., high in aromatic and phenolic content^{64,100–102}) was more likely to enhance bisphenol A oxidation. Second, in the divalent cation testing, bisphenol A oxidation was enhanced in the DL1 system at the low and moderate divalent cation concentrations compared to DOM-free controls. Therefore, we hypothesized DOM composition, specifically DOM of terrestrial origin and high in phenolic content, influenced the observed rate enhancement of bisphenol A.

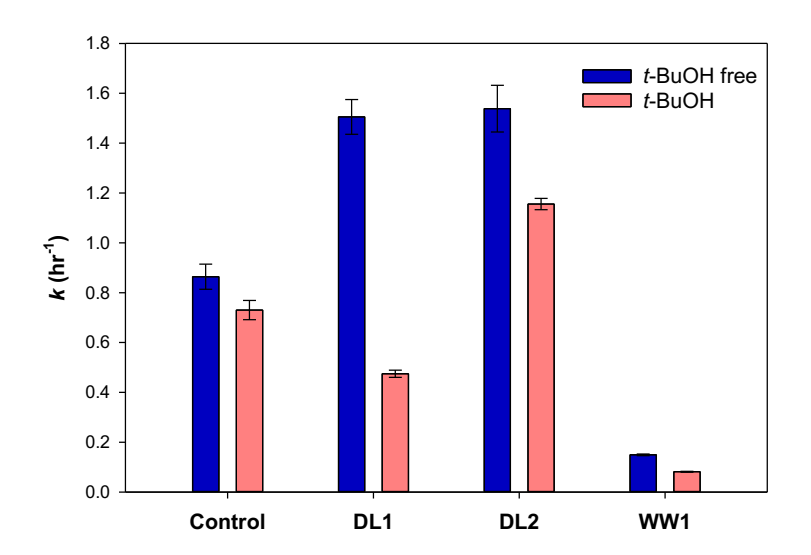


Figure 4. Pseudo-first order reaction rates for bisphenol A reacted in buffered (pH 5.5) ultrapure water (control), DL1 water, DL2 water, and WW1, with acid birnessite (1.70 mg; 0.39 mM-Mn) in the presence and absence of the radical quencher, *tert*-butanol (50 mM). Percent changes are presented in **Figure S8**. Error bars are the propagated standard error of the pseudo-first-order rate constants of triplicate reactors. Differences between *t*-BuOH-free and *t*-BuOH systems for DL1 are statistically significant (*t*-test, p < 0.05).

We further hypothesized that the observed increases in bisphenol A oxidation were driven by interactions between radicals generated when DOM is oxidized by acid birnessite. The reaction of phenols with manganese oxides first generates a phenoxy radical intermediate by a one-electron transfer.^{4,5,8,11,21} As DOM is likely oxidized via phenolic moieties,^{38,52,58-60} this radical formation

is potentially a key intermediate in the DOM oxidation process as well. Previous work has proposed that radical intermediates from oxidized phenols^{38,52,57–60} or model compounds⁵⁶ can indirectly transform organic contaminants, thereby increasing the observed oxidation rate constants of target compounds. However, direct evidence for this mechanism has not been exhibited in the presence of DOM.

The influence of radical-mediated reactions on bisphenol A rate enhancement was tested using the non-specific radical quencher *tert*-butanol with water samples from DL1, DL2, and WW1. The dystrophic lake samples were chosen because they resulted in large increases in the oxidation rate constant for bisphenol A (**Figure 1a**), had low fluorescence index values (**Table 1**), and were high in phenolic content, as measured by EDC (**Table 1**). The WW1 sample was selected because it resulted in the largest decrease in bisphenol A oxidation due to the high abundance of divalent cations; we expected radical-mediated reactions to be negligible in this sample. No significant change (p = 0.231; *t*-test) in bisphenol A oxidation was observed with *tert*-butanol in a DOM-free control solution (**Figure 4**; **Table S15**), demonstrating that the quencher did not impact manganese oxide reactivity.

Radical-mediated mechanisms contributed to the rate enhancement of bisphenol A oxidation in the presence of DOM from DL1 (**Figures 4** and **S8**; **Table S15**). The bisphenol A oxidation rate constant increased by 74% in the DL1 system compared to the control, but decreased by 45% under the same conditions in the presence of *tert*-butanol. The switch from a large rate enhancement to a rate decrease provided two important insights into the mechanism. First, the ability of *tert*-butanol to prevent the rate enhancement observed in the presence of DOM indicated that DOM-generated radicals led to increased bisphenol A oxidation. Second, when the DOM-generated radicals were removed from the system, an inhibitory mechanism drove a 45% rate

decrease for bisphenol A oxidation. This rate decrease was likely not driven by divalent cations due to their low abundance in the diluted water sample (0.01 mM total divalent cations). Instead, it was likely determined by competition between bisphenol A and the DOM for the manganese oxide surface and/or reductive dissolution of the manganese oxide.^{9,25,46,47,104}

Changes to bisphenol A oxidation in the DL2 *tert*-butanol system were not as large as those observed in the DL1 *tert*-butanol system (**Figure 4**; **Table S15**). Bisphenol A oxidation was enhanced by 78% in the DL2 system, which was nearly identical to the DL1 sample. Unlike the DL1 quenched system, bisphenol A oxidation was still enhanced by 34% in the DL2 quenched system. The decrease in bisphenol A rate enhancement indicated DOM-generated radicals were partially responsible for the observed rate enhancement; however, the 34% rate enhancement in the quenched DL2 system suggested another mechanism was important for enhancing bisphenol A removal. This alternative mechanism of rate enhancement could be due to complexation of the DOM with Mn(II) generated from the reductive dissolution of the acid birnessite, which could prevent the adsorption of Mn(II) to the mineral surface and therefore decrease competition with bisphenol A for surface active sites and result in a promotive effect on bisphenol A oxidation (**Figure S1**). ^{48,50,104}

The changes to bisphenol A oxidation in quenched and unquenched WW1 samples were similar (**Figure 4**; **Table S15**). Bisphenol A oxidation decreased by 83% in the unquenched system and by 91% in the WW1 system containing *tert*-butanol relative to the controls. The similar decreases (p = 0.126; *t*-test) to the bisphenol A rate constant in these systems indicated radical-mediated reactions were only important in systems where rate enhancement was observed. Thus, this system was likely dominated by the cation inhibition mechanism due to the high concentration

of divalent cations (1.73 mM total divalent cations) present in the diluted WW1 sample and any interactions with DOM were negligible.

Environmental Implications

Natural water constituents dramatically alter the oxidation of phenolic compounds by manganese oxides. The oxidation rate constants of the six target compounds in this study varied extensively depending on water chemistry (**Figure 1**). Furthermore, these changes were the result of combined interactions between DOM, divalent cations, and the target compound. Caution should be taken when comparing oxidation rate constants measured in simple, laboratory systems to real-world applications as oxidation kinetics can vary extensively in more complex systems.

Divalent cations and DOM are ubiquitous throughout natural and engineered systems and interact with other species in solutions, such as phenolic contaminants. We showed that divalent cations are a primary inhibitor of phenolic contaminant oxidation; however, the extent of divalent cation interaction can be dependent on the presence and composition of DOM (Figure 3). Furthermore, we demonstrated radical intermediates produced by DOM oxidation were primarily responsible for the observed increases in phenolic contaminant removal (Figure 4). This mechanism was dependent on DOM composition and was most significant in systems with DOM of primarily terrestrial origin (i.e., the dystrophic lakes).

The changes driven by divalent cations and DOM that impact phenolic contaminant transformation demonstrate the complexity of predicting the fate of such contaminants in complex systems. While previous work has focused on simple systems and individual species, we demonstrate the necessity to expand these investigations to more complex systems to predict the fate of these organic contaminants more accurately. For example, phenolic contaminants are likely

to degrade more slowly in a wastewater system than what would be predicted in a buffered, ultrapure water system in the laboratory. Conversely, some contaminants may degrade faster in systems that contain DOM that is similar to the DOM from the dystrophic lakes in this study. Importantly, phenol structure influences its reactivity with manganese oxides^{5,6,105,106} and therefore the impact of water constituents will vary among different phenols. Future work should seek to further explore how interactions between divalent cations and DOM affect contaminant transformation in environmentally relevant systems, particularly with DOM of diverse compositions. By studying these interactions in more complex systems, we can begin to understand how the transformation of these contaminants occurs in environmentally relevant systems.

Acknowledgements

This material is based upon work supported by the National Science Foundation (DGE-1747503 and CBET-1944464). Any opinions, findings, and conclusions or recommendations expressed in this material are those of the authors and do not necessarily reflect the views of the National Science Foundation. The authors thank Amber White for helping with sample collection and AnnaBeth Thomas for collecting the XRD spectra of the acid birnessite. The authors thank the Madison Metropolitan Sewerage District for assistance in collecting a secondary effluent sample.

Supporting Information

Additional experimental details, including water and DOM characterization, kinetic rates, and single linear regression outputs are included in the Supporting Information.

482 References

494

495

496

497

498

499

500

501

502

503

504

505

506

507

508

509

510

- 483 (1) Borch, T.; Kretzschmar, R.; Skappler, A.; Van Cappellen, P.; Ginder-Vogel, M.; Voegelin, A.; 484 Campbell, K. Biogeochemical redox processes and their impact on contaminant dynamics. *Environ. Sci. Technol.* **2010**, *44* (1), 15–23.
- 486 (2) Negra, C.; Ross, D. S.; Lanzirotti, A. Oxidizing behavior of soil manganese: Interactions among abundance, oxidation state, and pH. *Soil Sci. Soc. Am. J.* **2005**, *69*, 87–95.
- 488 (3) Nielsen-Franco, D.; Ginder-Vogel, M. Kinetic study of the influence of humic acids on the oxidation of As(III) by acid birnessite. *ACS ES&T Water* **2023**, *3*(4), 1060-1070.
- 490 (4) Remucal, C. K.; Ginder-Vogel, M. A critical review of the reactivity of manganese oxides with organic contaminants. *Environ. Sci. Process. Impacts* **2014**, *16*, 1247–1266.
- 492 (5) Stone, A. T. Reductive Dissolution of Manganese(III/IV) Oxides by Substituted Phenols. 493 *Environ. Sci. Technol.* **1987**, *21* (17), 979–988.
 - (6) Trainer, E. L.; Ginder-Vogel, M.; Remucal, C. K. Organic structure and solid characteristics determine reactivity of phenolic compounds with synthetic and reclaimed manganese oxides. *Environ. Sci. Water Res. Technol.* **2020**, *6* (3), 540–553.
 - (7) Balgooyen, S.; Alaimo, P. J.; Remucal, C. K.; Ginder-Vogel, M. Structural transformation of MnO₂ during the oxidation of bisphenol A. *Environ. Sci. Technol.* **2017**, *51* (11), 6053–6062.
 - (8) Stone, A. T.; Morgan, J. J.; Keck, W. M. Reduction and dissolution of manganese(III) and manganese(IV) oxides by organics: 2. Survey of the reactivity of organics. *Environ. Sci. Technol.* **1984**, *18*, 617–624.
 - (9) Klausen, J.; Haderlein, B. S.; Schwarzenbach, P. R. Oxidation of substituted anilines by aqueous MnO²: Effect of co-solutes on initial and quasi-steady-state kinetics. *Environ. Sci. Technol.* **1997**, *31*, 2642–2649.
 - (10) Chen, W. R.; Ding, Y.; Johnston, C. T.; Teppen, B. J.; Boyd, S. A.; Li, H. Reaction of lincosamide antibiotics with manganese oxide in aqueous solution. *Environ. Sci. Technol.* **2010**, *44* (12), 4486–4492.
 - (11) Shaikh, N.; Zhang, H.; Rasamani, K.; Artyushkova, K.; Ali, A. M. S.; Cerrato, J. M. Reaction of bisphenol A with synthetic and commercial MnO_{x(s)}: Spectroscopic and kinetic study. *Environ. Sci. Process. Impacts* **2018**, *20* (7), 1046–1055.
- 512 (12) Balgooyen, S.; Campagnola, G.; Remucal, C. K.; Ginder-Vogel, M. Impact of bisphenol A 513 influent concentration and reaction time on MnO₂ transformation in a stirred flow reactor. 514 *Environ. Sci. Process. Impacts* **2019**, *21* (1), 19–27.
- 515 (13) Lin, K.; Peng, Y.; Huang, X.; Ding, J. Transformation of bisphenol A by manganese oxide-516 coated sand. *Environ. Sci. Pollut. Res.* **2013**, *20* (3), 1461–1467.
- (14) Charbonnet, J. A.; Duan, Y.; Van Genuchten, C. M.; Sedlak, D. L. Chemical regeneration of manganese oxide-coated sand for oxidation of organic stormwater contaminants. *Environ. Sci. Technol.* 2018, 52 (18), 10728–10736.
- 520 (15) Grebel, J. E.; Charbonnet, J. A.; Sedlak, D. L. Oxidation of organic contaminants by 521 manganese oxide geomedia for passive urban stormwater treatment systems. *Water Res.* 522 **2016**, 88, 481–491.
- 523 (16) R. Masoner, J.; W. Kolpin, D.; T. Furlong, E.; M. Cozzarelli, I.; L. Gray, J.; A. Schwab, E. Contaminants of emerging concern in fresh leachate from landfills in the conterminous United States. *Environ. Sci. Process. Impacts* **2014**, *16* (10), 2335–2354.

- 526 (17) Baldwin, A. K.; Corsi, S. R.; De Cicco, L. A.; Lenaker, P. L.; Lutz, M. A.; Sullivan, D. J.; 527 Richards, K. D. Organic contaminants in great lakes tributaries: Prevalence and potential 528 aquatic toxicity. *Sci. Total Environ.* **2016**, *554*–*555*, 42–52.
- 529 (18) Belfroid, A.; van Velzen, M.; van der Horst, B.; Vethaak, D. Occurrence of bisphenol A in surface water and uptake in fish: Evaluation of field measurements. *Chemosphere* **2002**, *49* (1), 97–103.
- 532 (19) Kitamura, S.; Suzuki, T.; Sanoh, S.; Kohta, R.; Jinno, N.; Sugihara, K.; Yoshihara, S.; Fujimoto, N.; Watanabe, H.; Ohta, S. Comparative study of the endocrine-disrupting activity of bisphenol A and 19 related compounds. *Toxicol. Sci. Off. J. Soc. Toxicol.* **2005**, 84 (2), 249–259.
- 536 (20) Soares, A.; Guieysse, B.; Jefferson, B.; Cartmell, E.; Lester, J. N. Nonylphenol in the environment: A critical review on occurrence, fate, toxicity and treatment in wastewaters.

 538 *Environ. Int.* **2008**, *34* (7), 1033–1049.
- 539 (21) Luther, G. W. Manganese(II) oxidation and Mn(IV) reduction in the environment two oneelectron transfer steps versus a single two-electron step. *Geomicrobiol. J.* **2005**, *22* (3–4), 541 195–203.
- 542 (22) Gao, N.; Hong, J.; Yu, Z.; Peng, P.; Huang, W. Transformation of bisphenol A in the presence of manganese dioxide. *Soil Sci.* **2011**, *176* (6), 265–272.
- 544 (23) Lin, K.; Liu, W.; Gan, J. Oxidative removal of bisphenol A by manganese dioxide: Efficacy, products, and pathways. *Environ. Sci. Technol.* **2009**, *43* (10), 3860–3864.
- 546 (24) Lu, Z.; Gan, J. Oxidation of nonylphenol and octylphenol by manganese dioxide: Kinetics and pathways. *Environ. Pollut.* **2013**, *180*, 214–220.
- 548 (25) Zhang, H.; Huang, C. H. Oxidative transformation of triclosan and chlorophene by manganese oxides. *Environ. Sci. Technol.* **2003**, *37* (11), 2421–2430.
- 550 (26) Balgooyen, S.; Remucal, C. K.; Ginder-Vogel, M. Identifying the mechanisms of cation inhibition of phenol oxidation by acid birnessite. *J. Environ. Qual.* **2020**, *49* (6), 1644–1654.
- 552 (27) Lin, K.; Yan, C.; Gan, J. Production of hydroxylated polybrominated diphenyl ethers (OH-553 PBDEs) from bromophenols by manganese dioxide. *Environ. Sci. Technol.* **2014**, *48* (1), 554 263–271.
- 555 (28) Lu, Z.; Lin, K.; Gan, J. Oxidation of bisphenol F (BPF) by manganese dioxide. *Environ. Pollut.* **2011**, *159* (10), 2546–2551.
- (29) Zhang, T.; Zhang, X.; Yan, X.; Ng, J.; Wang, Y.; Sun, D. D. Removal of bisphenol A via a
 hybrid process combining oxidation on β-MnO₂ nanowires with microfiltration. *Colloids* Surf. Physicochem. Eng. Asp. 2011, 392 (1), 198–204.
- 560 (30) Barrett, K. A.; McBride, M. B. Oxidative degradation of glyphosate and aminomethylphosphonate by manganese oxide. *Environ. Sci. Technol.* **2005**, *39* (23), 9223–9228.
- 563 (31) Murray, J. W. The interaction of metal ions at the manganese dioxide-solution interface. 564 *Geochim. Cosmochim. Acta* **1975**, *39* (4), 505–519.
- 565 (32) Allard, S.; Gutierrez, L.; Fontaine, C.; Croué, J. P.; Gallard, H. Organic matter interactions 566 with natural manganese oxide and synthetic birnessite. *Sci. Total Environ.* **2017**, *583*, 487– 567 495.
- 568 (33) Wang, Q.; Yang, P.; Zhu, M. Effects of metal cations on coupled birnessite structural transformation and natural organic matter adsorption and oxidation. *Geochim. Cosmochim.* 570 *Acta* **2019**, *250*, 292–310.

- 571 (34) Tipping, E.; Heaton, M. J. The adsorption of aquatic humic substances by two oxides of manganese. *Geochim. Cosmochim. Acta* **1983**, *47*, 1393–1397.
- 573 (35) Liu, R.; Liu, H.; Qiang, Z.; Qu, J.; Li, G.; Wang, D. Effects of calcium ions on surface characteristics and adsorptive properties of hydrous manganese dioxide. *J. Colloid Interface Sci.* **2009**, *331* (2), 275–280.
- 576 (36) Baham, J.; Sposito, G. Adsorption of dissolved organic carbon extracted from sewage sludge 577 on montmorillonite and kaolinite in the presence of metal ions. *J. Environ. Qual.* **1994**, *23* 578 (1), 147–153.
- 579 (37) Santschi, P. H.; Lenhart, J. J.; Honeyman, B. D. Heterogeneous processes affecting trace contaminant distribution in estuaries: The role of natural organic matter. *Mar. Chem.* **1997**, 581 58, 99–125.
- 582 (38) Trainer, E. L.; Ginder-Vogel, M.; Remucal, C. K. Selective reactivity and oxidation of dissolved organic matter by manganese oxides. *Environ. Sci. Technol.* **2021**, *55* (17), 12084–12094.

586

587

588

589

590

591

592

593

594

595

596

597

600

601

- (39) Aiken, G. R.; Hsu-Kim, H.; Ryan, J. N. Influence of dissolved organic matter on the environmental fate of metals, nanoparticles, and colloids. *Environ. Sci. Technol.* **2011**, *45* (8), 3196–3201.
- (40) Berg, S. M.; Whiting, Q. T.; Herrli, J. A.; Winkels, R.; Wammer, K. H.; Remucal, C. K. The role of dissolved organic matter composition in determining photochemical reactivity at the molecular level. *Environ. Sci. Technol.* **2019**, *53* (20), 11725–11734.
- (41) Maizel, A. C.; Remucal, C. K. Molecular composition and photochemical reactivity of size-fractionated dissolved organic matter. *Environ. Sci. Technol.* **2017**, *51* (4), 2113–2123.
- (42) McElmurry, S. P.; Long, D. T.; Voice, T. C. Stormwater dissolved organic matter: Influence of land cover and environmental factors. *Environ. Sci. Technol.* **2014**, *48* (1), 45–53.
- (43) Minor, E. C.; Swenson, M. M.; Mattson, B. M.; Oyler, A. R. Structural characterization of dissolved organic matter: A review of current techniques for isolation and analysis. *Environ. Sci. Process. Impacts* **2014**, *16* (9), 2064–2079.
- 598 (44) Zhang, H.; Chen, W. R.; Huang, C. H. Kinetic modeling of oxidation of antibacterial agents 599 by manganese oxide. *Environ. Sci. Technol.* **2008**, *42* (15), 5548–5554.
 - (45) Sun, K.; Li, S.; Waigi, M. G.; Huang, Q. Nano-MnO₂-mediated transformation of triclosan with humic molecules present: Kinetics, products, and pathways. *Environ. Sci. Pollut. Res. Int.* **2018**, *25* (15), 14416–14425.
- 603 (46) Kang, K. H.; Dec, J.; Park, H.; Bollag, J. M. Effect of phenolic mediators and humic acid on cyprodinil transformation in presence of birnessite. *Water Res.* **2004**, *38* (11), 2737–2745.
- 605 (47) Tran, T. H.; Labanowski, J.; Gallard, H. Adsorption and transformation of the anthelmintic drug niclosamide by manganese oxide. *Chemosphere* **2018**, *201*, 425–431.
- (48) Kim, D.-G.; Jiang, S.; Jeong, K.; Ko, S.-O. Removal of 17α-ethinylestradiol by biogenic
 manganese oxides produced by the *Pseudomonas putida* strain MnB1. *Water. Air. Soil Pollut.* 2012, 223 (2), 837–846.
- 610 (49) He, Y.; Xu, J.; Zhang, Y.; Guo, C.; Li, L.; Wang, Y. Oxidative transformation of carbamazepine by manganese oxides. *Environ. Sci. Pollut. Res.* **2012**, *19* (9), 4206–4213.
- 612 (50) Xu, L.; Xu, C.; Zhao, M.; Qiu, Y.; Sheng, G. D. Oxidative removal of aqueous steroid estrogens by manganese oxides. *Water Res.* **2008**, *42* (20), 5038–5044.
- 614 (51) Feitosa-Felizzola, J.; Hanna, K.; Chiron, S. Adsorption and transformation of selected 615 human-used macrolide antibacterial agents with iron(III) and manganese(IV) oxides. 616 *Environ. Pollut.* **2009**, *157* (4), 1317–1322.

- 617 (52) Yang, B.; Du, P.; Chen, G.; Zhang, P.; Zhang, Q.; Wang, Z.; Zhang, G.; Cai, Z.; Wang, J. Dual role of soil-derived dissolved organic matter in the sulfamethoxazole oxidation by manganese dioxide. *Water Res.* **2023**, *235*, 119901.
- 620 (53) Sunda, W. G.; Huntsman, S. A.; Harvey, G. R. Photoreduction of manganese oxides in seawater and its geochemical and biological implications. *Nature* **1983**, *301* (5897), 234–622 236.
- 623 (54) Bertlnot, D. J.; Zepp, R. G. Effects of solar radiation on manganese oxide reactions with selected organic compounds. *Env. Sci Technol* **1991**, *25*, 1267–1273.
- 625 (55) Bialk, H. M.; Simpson, A. J.; Pedersen, J. A. Cross-coupling of sulfonamide antimicrobial agents with model humic constituents. *Environ. Sci. Technol.* **2005**, *39* (12), 4463–4473.
- 627 (56) Song, Y.; Jiang, J.; Ma, J.; Zhou, Y.; von Gunten, U. Enhanced transformation of sulfonamide 628 antibiotics by manganese(IV) oxide in the presence of model humic constituents. *Water Res.* 629 **2019**, *153*, 200–207.
- 630 (57) Trainer, E. L.; Ginder-Vogel, M.; Remucal, C. K. Enhancement and inhibition of oxidation in phenolic compound mixtures with manganese oxides. *ACS ES&T Water* **2022**, *2* (12), 2400–2408.
- 633 (58) Zhang, J.; McKenna, A. M.; Zhu, M. Macromolecular characterization of compound 634 selectivity for oxidation and oxidative alterations of dissolved organic matter by manganese 635 oxide. *Environ. Sci. Technol.* **2021**, *55* (11), 7741–7751.
- 636 (59) Ding, Z.; Ding, Y.; Liu, F.; Yang, J.; Li, R.; Dang, Z.; Shi, Z. Coupled sorption and oxidation 637 of soil dissolved organic matter on manganese oxides: Nano/sub-nanoscale distribution and 638 molecular transformation. *Environ. Sci. Technol.* **2022**, *56* (4), 2783–2793.
- 639 (60) Guo, B.; Wang, J.; Sathiyan, K.; Ma, X.; Lichtfouse, E.; Huang, C.-H.; Sharma, V. K. 640 Enhanced oxidation of antibiotics by ferrate mediated with natural organic matter: Role of 641 phenolic moieties. *Environ. Sci. Technol.* **2023**, *57*(47), 19033-19042.
- (61) Berg, S. M.; Mooney, Robert J.; McConville, Megan B.; McIntyre, Peter B.; Remucal, C. K.
 Seasonal and spatial variability of dissolved carbon concentration and composition in lake
 michigan tributaries. *J. Geophys. Res. Biogeosciences* 2021, *126*.
- 645 (62) Berg, S. M.; Peterson, B. D.; McMahon, K. D.; Remucal, C. K. Spatial and temporal variability of dissolved organic matter molecular composition in a stratified eutrophic lake.

 J. Geophys. Res. Biogeosciences 2022, 127 (1), e2021JG006550.
- 648 (63) Berg, S. M.; Wammer, K. H.; Remucal, C. K. Dissolved organic matter photoreactivity is determined by its optical properties, redox activity, and molecular composition. *Environ. Sci. Technol.* **2023**, *57*(16), 6703-6711
- (64) Maizel, A. C.; Li, J.; Remucal, C. K. Relationships between dissolved organic matter
 composition and photochemistry in lakes of diverse trophic status. *Environ. Sci. Technol.* 2017, 51 (17), 9624–9632.
- 654 (65) Milstead, R. P.; Horvath, E. R.; Remucal, C. K. Dissolved organic matter composition 655 determines its susceptibility to complete and partial photooxidation within lakes. *Environ.* 656 *Sci. Technol.* **2023**, *57* (32), 11876–11885.
- 657 (66) Bulman, D. M.; Remucal, C. K. Role of reactive halogen species in disinfection byproduct formation during chlorine photolysis. *Environ. Sci. Technol.* **2020**, *54* (15), 9629–9639.
- 659 (67) Milstead, R. P.; Remucal, C. K. Molecular-level insights into the formation of traditional and novel halogenated disinfection byproducts. *ACS ES&T Water* **2021**, *1* (8), 1966–1974.

- 661 (68) Remucal, C. K.; Salhi, E.; Walpen, N.; von Gunten, U. Molecular-level transformation of dissolved organic matter during oxidation by ozone and hydroxyl radical. *Environ. Sci. Technol.* **2020**, *54* (16), 10351–10360.
- 664 (69) Wallace, G. C.; Sander, M.; Chin, Y. P.; Arnold, W. A. Quantifying the electron donating capacities of sulfide and dissolved organic matter in sediment pore waters of wetlands. *Environ. Sci. Process. Impacts* **2017**, *19* (5), 758–767.
- (70) Walpen, N.; Getzinger, G. J.; Schroth, M. H.; Sander, M. Electron-donating phenolic and electron-accepting quinone moieties in peat dissolved organic matter: Quantities and redox transformations in the context of peat biogeochemistry. *Environ. Sci. Technol.* 2018, 52 (9), 5236–5245.
- 671 (71) Wenk, J.; Aeschbacher, M.; Salhi, E.; Canonica, S.; Von Gunten, U.; Sander, M. Chemical oxidation of dissolved organic matter by chlorine dioxide, chlorine, and ozone: Effects on its optical and antioxidant properties. *Environ. Sci. Technol.* **2013**, *47* (19), 11147–11156.
- 674 (72) Costentin, C.; Robert, M.; Savéant, J.-M. Concerted proton-electron transfers: Electrochemical and related approaches. *Acc. Chem. Res.* **2010**, *43* (7), 1019–1029.
- 676 (73) Salter-Blanc, A. J.; Bylaska, E. J.; Lyon, M. A.; Ness, S. C.; Tratnyek, P. G. Structure-activity 677 relationships for rates of aromatic amine oxidation by manganese dioxide. *Environ. Sci.* 678 *Technol.* **2016**, *50* (10), 5094–5102.
- 679 (74) Hansch, Corwin.; Leo, A.; Taft, R. W. A survey of hammett substituent constants and resonance and field parameters. *Chem. Rev.* **1991**, *91* (2), 165–195.
- 681 (75) Tratnyek, P. G.; Weber, E. J.; Schwarzenbach, R. P. Quantitative structure-activity relationships for chemical reductions of organic contaminants. *Environ. Toxicol. Chem.* **2003**, *22* (8), 1733–1742.

685

686

- (76) Canonica, S.; Tratnyek, P. G. Quantitative structure-activity relationships for oxidation reactions of organic chemicals in water. *Environ. Toxicol. Chem.* **2003**, *22* (8), 1743–1754.
- (77) McKenzie, R. M. The synthesis of birnessite, cryptomelane, and some other oxides and hydroxides of manganese. *Mineral. Mag.* **1971**, *38* (296), 493–502.
- 688 (78) Ohlweiler, O. A.; Schneider, A. M. H. Standardization of potassium permanganate by titration of sodium oxalate in presence of perchloric acid and manganese(II) sulfate. *Anal. Chim. Acta* **1972**, *58* (2), 477–480.
- 691 (79) Weishaar, J. L.; Aiken, G. R.; Bergamaschi, B. A.; Fram, M. S.; Fujii, R.; Mopper, K. Evaluation of specific ultraviolet absorbance as an indicator of the chemical composition and reactivity of dissolved organic carbon. *Environ. Sci. Technol.* **2003**, *37* (20), 4702–4708.
- 694 (80) Helms, J. R.; Stubbins, A.; Ritchie, J. D.; Minor, E. C.; Kieber, D. J.; Mopper, K. Absorption 695 spectral slopes and slope ratios as indicators of molecular weight, source, and 696 photobleaching of chromophoric dissolved organic matter. *Limnol. Oceanogr.* **2008**, *53* (3), 697 955–969.
- 698 (81) McKnight, D. M.; Boyer, E. W.; Westerhoff, P. K.; Doran, P. T.; Kulbe, T.; Andersen, D. T. Spectrofluorometric characterization of dissolved organic matter for indication of precursor organic material and aromaticity. *Limnol. Oceanogr.* **2001**, *46* (1), 38–48.
- 701 (82) Cory, R. M.; Miller, M. P.; McKnight, D. M.; Guerard, J. J.; Miller, P. L. Effect of instrument-702 specific response on the analysis of fulvic acid fluorescence spectra. *Limnol. Oceanogr.* 703 *Methods* **2010**, 8 (2), 67–78.
- 704 (83) Hansen, A. M.; Kraus, T. E. C.; Pellerin, B. A.; Fleck, J. A.; Downing, B. D.; Bergamaschi, 705 B. A. Optical properties of dissolved organic matter (DOM): Effects of biological and 706 photolytic degradation. *Limnol. Oceanogr.* **2016**, *61* (3), 1015–1032.

- 707 (84) Stauffer, R. E. Cycling of manganese and iron in Lake Mendota, Wisconsin. *Environ. Sci. Technol.* **1986**, *20* (5), 449–457.
- 709 (85) Schacht, L.; Ginder-Vogel, M. Arsenite depletion by manganese oxides: A case study on the limitations of observed first order rate constants. *Soil Syst.* **2018**, *2* (3), 39.
- (86) Balistrieri, L. S.; Murray, J. W. The surface chemistry of δ-MnO₂ in major ion sea water.
 Geochim. Cosmochim. Acta 1982, 46 (6), 1041–1052.
- 713 (87) Gao, J.; Duan, X.; O'Shea, K.; Dionysiou, D. D. Degradation and transformation of bisphenol 714 A in UV/sodium percarbonate: Dual role of carbonate radical anion. *Water Res.* **2020**, *171*, 715 115394.
- 716 (88) Liu, J.; An, F.; Li, M.; Yang, L.; Wan, J.; Zhang, S. Efficient degradation of 2,4-717 dichlorophenol on activation of peroxymonosulfate mediated by MnO₂. *Bull. Environ.* 718 *Contam. Toxicol.* **2021**, *107* (2), 255–262.

720

- (89) Shahamat, Y. D.; Farzadkia, M.; Nasseri, S.; Mahvi, A. H.; Gholami, M.; Esrafili, A. Magnetic heterogeneous catalytic ozonation: A new removal method for phenol in industrial wastewater. *J. Environ. Health Sci. Eng.* **2014**, *12* (1), 50.
- 722 (90) Huang, J.; Dai, Y.; Singewald, K.; Liu, C.-C.; Saxena, S.; Zhang, H. Effects of MnO₂ of 723 different structures on activation of peroxymonosulfate for bisphenol A degradation under 724 acidic conditions. *Chem. Eng. J.* **2019**, *370*, 906–915.
- 725 (91) Zhang, P.; Zhang, G.; Dong, J.; Fan, M.; Zeng, G. Bisphenol A oxidative removal by ferrate (Fe(VI)) under a weak acidic condition. *Sep. Purif. Technol.* **2012**, *84*, 46–51.
- 727 (92) Arnold, W. A.; Oueis, Y.; O'Connor, M.; Rinaman, J. E.; Taggart, M. G.; McCarthy, R. E.; Foster, K. A.; Latch, D. E. QSARs for phenols and phenolates: Oxidation potential as a predictor of reaction rate constants with photochemically produced oxidants. *Environ. Sci. Process. Impacts* **2017**, *19* (3), 324–338.
- 731 (93) Pavitt, A. S.; Bylaska, E. J.; Tratnyek, P. G. Oxidation potentials of phenols and anilines:
 Correlation analysis of electrochemical and theoretical values. *Environ. Sci. Process.*733 *Impacts* **2017**, *19* (3), 339–349.
- 734 (94) Villalobos, M.; Escobar-Quiroz, I. N.; Salazar-Camacho, C. The influence of particle size 735 and structure on the sorption and oxidation behavior of birnessite: I. Adsorption of As(V) 736 and oxidation of As(III). *Geochim. Cosmochim. Acta* **2014**, *125*, 564–581.
- 737 (95) Kwon, K. D.; Refson, K.; Sposito, G. Understanding the trends in transition metal sorption 738 by vacancy sites in birnessite. *Geochim. Cosmochim. Acta* **2013**, *101*, 222–232.
- 739 (96) Johnson, K.; Purvis, G.; Lopez-Capel, E.; Peacock, C.; Gray, N.; Wagner, T.; März, C.; Bowen, L.; Ojeda, J.; Finlay, N.; Robertson, S.; Worrall, F.; Greenwell, C. Towards a mechanistic understanding of carbon stabilization in manganese oxides. *Nat. Commun.* 2015, 6.
- 743 (97) Walpen, N.; Houska, J.; Salhi, E.; Sander, M.; von Gunten, U. Quantification of the electron 744 donating capacity and UV absorbance of dissolved organic matter during ozonation of 745 secondary wastewater effluent by an assay and an automated analyzer. *Water Res.* **2020**, 746 185, 116235.
- 747 (98) Fimmen, R. L.; Cory, R. M.; Chin, Y. P.; Trouts, T. D.; McKnight, D. M. Probing the oxidation-reduction properties of terrestrially and microbially derived dissolved drganic Matter. *Geochim. Cosmochim. Acta* **2007**, *71* (12), 3003–3015.
- 750 (99) Cory, R. M.; McKnight, D. M. Fluorescence spectroscopy reveals ubiquitous presence of oxidized and reduced quinones in dissolved organic matter. *Environ. Sci. Technol.* **2005**, *39* (21), 8142–8149.

- 753 (100) Mostovaya, A.; Koehler, B.; Guillemette, F.; Brunberg, A.-K.; Tranvik, L. J. Effects of compositional changes on reactivity continuum and decomposition kinetics of lake dissolved organic matter. *J. Geophys. Res. Biogeosciences* **2016**, *121* (7), 1733–1746.
- 756 (101) Müller, M. B.; Schmitt, D.; Frimmel, F. H. Fractionation of natural organic matter by size exclusion chromatography–properties and stability of fractions. *Environ. Sci. Technol.* **2000**, *34* (23), 4867–4872.
- 759 (102) Minor, E.; Stephens, B. Dissolved organic matter characteristics within the Lake Superior watershed. *Org. Geochem.* **2008**, *39* (11), 1489–1501.
- 761 (103) Aeschbacher, M.; Graf, C.; Schwarzenbach, R. P.; Sander, M. Antioxidant properties of humic substances. *Environ. Sci. Technol.* **2012**, *46* (9), 4916–4925.

- (104) Zhu, M.-X.; Wang, Z.; Xu, S.-H.; Li, T. Decolorization of methylene blue by δ-MnO₂-coated montmorillonite complexes: Emphasizing redox reactivity of Mn-oxide coatings. *J. Hazard. Mater.* **2010**, *181* (1–3), 57–64.
- (105) Ulrich, H.-J.; Stone, A. T. Oxidation of chlorophenols adsorbed to manganese oxide surfaces. *C Visibility Prot. Res. Policy Asp.* **1989**, *23* (7), 2231–2244.
- (106) Park, J.-W.; Dec, J.; Kim, J.-E.; Bollag, J.-M. Effect of humic constituents on the transformation of chlorinated phenols and anilines in the presence of oxidoreductive enzymes or birnessite. *Environ. Sci. Technol.* **1999**, *33* (12), 2028–2034.